This is an Author Accepted Manuscript version of the following article: D. Cilden-Guler, Z. Kaymaz, C. Hajiyev, Geomagnetic Storms in the Context of Spacecraft Attitude Estimation under Different Noise Levels. Advances in Space Research, 72(7), pp. 2733-2740, DOI: 10.1016/j.asr.2022.09.021, 2023.

Geomagnetic Storms in the Context of Spacecraft Attitude Estimation under Different Noise Levels

Demet Cilden-Guler[1,*], Zerefsan Kaymaz[2], and Chingiz Hajiyev[3]

Abstract

This study examines geomagnetic storm conditions for attitude estimation of a spacecraft having magnetometers with various measurement noise levels at low Earth orbit. The geomagnetic field models are introduced by taking the external field effects into account. It is important to discuss the limitations of the models and the measurements that are being used. Therefore, the external effects are evaluated under different noise levels of magnetometer to determine and discuss the suppression level caused by the noise levels in a general framework. External magnetic field effects are examined by the ratio to noise under various magnetometer standard deviations up to 300 nT. An analysis is carried out for attitude estimation using Kalman-type filter in order to determine what noise level is acceptable on a particular sensor with a specified attitude requirement, magnetic field model, and space weather conditions.

This study indicates that external magnetic fields are vital for establishing attitude processes based on magnetometers with varying noise on which the spacecraft relies for accuracy.

Keywords: Geomagnetic storm, Attitude estimation, Magnetometer noise, Spacecraft.

1. Introduction

Spacecraft or their instruments are controlled for maintaining their orientation to specified points or directions. To control the craft or the device, the attitude needs to be estimated during flight. There are several sensors that can be used for satellites in low Earth orbit (LEO). One of the most widely used attitude sensor is the magnetometers as they are cheap, commercial off-the-shelf, light, and reliable sensors. However, they may be affected by the electronic devices on the satellite and, therefore, placed away from the satellite body on a boom. The magnetometers implemented on a LEO satellite to measure the internal geomagnetic field sources caused by the Earth's dynamo and crust as well as the external sources such as those created by interplanetary magnetic field and solar

[*] Corresponding Author.

[1]Assistant Professor at Astronautical Engineering Department, Istanbul Technical University, Istanbul, Turkey, e-mail: cilden@itu.edu.tr, https://orcid.org/0000-0002-3924-5422.

[2]Professor, Meteorological Engineering Department, Faculty of Aeronautics and Astronautics, Istanbul Technical University, Istanbul, Turkey, e-mail: zerefsan@itu.edu.tr, https://orcid.org/0000-0002-9289-9767.

[3]Professor, Aeronautical Engineering Department, Faculty of Aeronautics and Astronautics, Istanbul Technical University, Istanbul, Turkey, e -mail: cingiz@itu.edu.tr, https://orcid.org/0000-0003-4115-341X.

wind. In attitude determination and control systems, the International Geomagnetic Reference Field (IGRF) (Thébault et al., 2015) is frequently used as the major magnetic field model. Yet, it might remain incapable when geomagnetic activities occur, which can produce an error in the magnetic field model in comparison with the sensor measurements. At this point, it is important to study the effects of the geomagnetic storms on the spacecraft (Cui et al., 2020; Lu et al., 2019).

The external magnetic field variations caused by solar wind and magnetic storms and magnetospheric substorms are generally treated as bias on the measurements, and removed from the measurements by estimating them in the augmented states (Inamori et al., 2016; Inamori and Nakasuka, 2012). The measurements in this case deviate from the real case after the elimination. Another approach to reduce the errors resulting from the external fields is to consider the external field in the geomagnetic model and not treat it as an error source (Cilden-Guler et al., 2021, 2018). By this way, the geomagnetic model can represent the magnetic field closer to the reality. If the magnetic field model used for the satellite attitude control does not consider the external fields, it can misevaluate that there is more noise on the sensor, while actually the variations are caused by a physical phenomenon (e.g. a magnetospheric substorm event), not from the sensor itself. That is why, in this study, another geomagnetic field model in addition to the IGRF model is introduced, which is called T89 (Tsyganenko, 1989) for modeling the geomagnetic field and simulating the magnetometer better within the context of the spacecraft attitude estimation.

Many of the error sources such as bias on the magnetometer measurements may be compensated during the ground tests prior to the spacecraft launch or during in-orbit calibration after launch. In this research, the magnetometers are assumed to be calibrated against biases and scaling errors. On the other hand, the measurement noise is present in the magnetometers as in all other sensors. The standard deviation of magnetometer measurement noise in small satellites may vary depending on the chosen sensor such as ~3 nT (Olsen et al., 2020), 40 nT (Cui et al., 2020), 100 nT (Zhang et al., 2015), ~200 nT (Schulz et al., 2019), 200 nT (Carletta et al., 2020), 300 nT (Soken and Sakai, 2020). According to the literature, the standard deviations of magnetometers might vary by as much as two orders of magnitude. This could be due to the magnetometer's required parameters such as cost, size, weight, accuracy, and so on for a certain mission. This variation may result in having a large error source from the sensor itself. If the noise on the magnetometer is large enough, the external field might be suppressed and not revealed in the magnetic field observations. Therefore, the critical noise levels masking the external fields are discussed for one magnetically active event in (Cilden-Guler et al., 2019), and for an attitude estimation algorithm in the follow-up study (Cilden-Guler et al., 2020). The purpose of this paper, on the other hand, is to evaluate these issues in detail and to give a general framework in determining which model to be used at which noise level case for attitude estimation applications. For this purpose, an extensive analysis is carried out under various magnetic activity and magnetometer noise levels.

The rest of the paper is composed of,

- Mathematical model for the spacecraft’s rotational motion,

This is an Author Accepted Manuscript version of the following article: D. Cilden-Guler, Z. Kaymaz, C. Hajiyev, Geomagnetic Storms in the Context of Spacecraft Attitude Estimation under Different Noise Levels. Advances in Space Research, 72(7), pp. 2733-2740, DOI: 10.1016/j.asr.2022.09.021, 2023.

- Description of the geomagnetic field models,
- Mathematical model for the magnetometer measurements,
- Attitude estimation algorithm based on Kalman type filtering,
- Analysis and results of case studies,
- Discussion and conclusions based on the analysis and results.

2. Mathematical Models

The mathematical models used in the estimation filter is given in this section. The spacecraft's rotational motion is used in the process model of the estimation filter and in modeling the actual dynamics of the spacecraft within the simulation. The geomagnetic field model is utilized in filter as a reference model and in modeling the magnetometer measurements.

2.1. Spacecraft's Rotational Motion

The spacecraft's attitude angles and angular rates are composing the state vector considered in this study. The attitude angles are represented by Euler angles by,

$$\begin{bmatrix} \dot{\phi} \\ \dot{\theta} \\ \dot{\psi} \end{bmatrix} = \begin{bmatrix} 1 & s(\phi)t(\theta) & c(\phi)t(\theta) \\ 0 & c(\phi) & -s(\phi) \\ 0 & s(\phi)/c(\theta) & c(\phi)/c(\theta) \end{bmatrix} \begin{bmatrix} p \\ q \\ r \end{bmatrix}. \tag{1}$$

Here cosine, sine and tangent functions are expressed by $c(\cdot)$, $s(\cdot)$, and $t(\cdot)$ respectively, vector of the angular velocity $(\boldsymbol{\omega}_{BR})$ in body coordinates with respect to the orbit coordinates has the components of p, q, r. Here, attitude problem is formulated using Euler angles as it is easy to visualize the three angles of rotation. However, it should be noted that Euler angles might be subject to singularity in some cases. Other attitude representations including quaternions and modified Rodriguez parameters can be used for a solution to the singularity issue. The angular velocity vector $(\boldsymbol{\omega}_{BI})$ in body coordinates with respect to the inertial frame can be expressed as,

$$\boldsymbol{\omega}_{BI} = \begin{bmatrix} \omega_x & \omega_y & \omega_z \end{bmatrix}^T, \tag{2}$$

The angular velocities ($\boldsymbol{\omega}_{BI}, \boldsymbol{\omega}_{BR}$) in body frame have a relationship,

$$\boldsymbol{\omega}_{BR} = \boldsymbol{\omega}_{BI} - \mathbf{A}\begin{bmatrix} 0 & -\omega_o & 0 \end{bmatrix}^T, \tag{3}$$

where ω_o is the orbital angular velocity and can be computed for the circular orbits as,

$$\omega_o = \left(\mu / r_0^3\right)^{1/2} \tag{4}$$

with μ gravitational constant, r_0 spacecraft-Earth distance. $\mathbf{A}$ is the attitude matrix transforming

This is an Author Accepted Manuscript version of the following article: D. Cilden-Guler, Z. Kaymaz, C. Hajiyev, Geomagnetic Storms in the Context of Spacecraft Attitude Estimation under Different Noise Levels. Advances in Space Research, 72(7), pp. 2733-2740, DOI: 10.1016/j.asr.2022.09.021, 2023.

the vectors from orbit to body coordinates.

Using the principle of the conservation of angular momentum, the dynamic equations are shown as,

$$J_x \frac{d\omega_x}{dt} = N_x + \left(J_y - J_z\right)\omega_y \omega_z, \tag{5}$$

$$J_y \frac{d\omega_y}{dt} = N_y + \left(J_z - J_x\right)\omega_z \omega_x, \tag{6}$$

$$J_z \frac{d\omega_z}{dt} = N_z + \left(J_x - J_y\right)\omega_x \omega_y. \tag{7}$$

Here, J_x, J_y and J_z are the elements of the moment of inertia matrix whereas the external disturbances are shown as N_x, N_y and N_z.

2.2. Geomagnetic Field Models

To determine the attitude angles of a satellite using magnetometer measurements, the estimation filter uses one of the geomagnetic field models. IGRF (International Geomagnetic Reference Field) is a commonly used geomagnetic field model and it computes the geomagnetic field vector using the inputs of date and position of the spacecraft orbiting around Earth (Thébault et al., 2015; Wertz, 2002). In the model, the magnetic field at a point in space is predicted using the spherical components as stated in Eq. (8) below:

$$\mathbf{B}_{\mathrm{IGRF}}(\bar{r}, \mathrm{colat}, \mathrm{lon}, t) = -\nabla\{a \sum_{n=1}^{N} \sum_{m=0}^{n} (\frac{a}{\bar{r}})^{n+1} [\mathrm{g}_n^m(\mathrm{t})\,\mathrm{c}\left(m\mathrm{lon}\right) + \mathrm{h}_n^m(\mathrm{t})\,\mathrm{s}\left(m\mathrm{lon}\right)] \times P_n^m(\mathrm{c}\left(\mathrm{colat}\right))\}, \tag{8}$$

where $\mathbf{B}_{\mathrm{IGRF}}$ represents the magnetic field vector prediction in nT, $\mathrm{colat}(t)$ is the co-latitude, $\mathrm{lon}(t)$ is the longitude, $\bar{r}$ is spacecraft-Earth mass centers' distance with $a = 6371.2$ km being the mean radius of Earth, P_n^m is the Schmidt quasi-normalized associated Legendre polynomials of degree n and order m, g_n^m and h_n^m are the Gaussian coefficients in nT (Thébault et al., 2015).

As IGRF model considers only the internal magnetic field, the real magnetometer measurements might be under predicted in the simulations since the external magnetic fields are not considered. In order to simulate the real physical space environment, the T89 model that consists both internal and external magnetic field sources is selected (Tsyganenko, 1989). T89 is composed of two parts as:

$$\mathbf{B}_{\mathrm{T89}_k} = \mathbf{B}_{\mathrm{IGRF}_k} + \mathbf{B}_{\mathrm{ext}_k}, \tag{9}$$

$$\mathbf{B}_{\mathrm{ext}} = \mathbf{B}_{ring} + \mathbf{B}_{tail} + \mathbf{B}_{mp} + \mathbf{B}_{FC}, \tag{10}$$

where $\mathbf{B}_{\mathrm{T89}}$ represents magnetic field vector of T89 model including the IGRF outputs $\left(\mathbf{B}_{\mathrm{IGRF}}\right)$ and external magnetic field contribution $\left(\mathbf{B}_{\mathrm{ext}}\right)$. IGRF model only considers the internal part of the geomagnetic field of Earth and updates its constants every five year (Thébault et al., 2015) whereas T89 model uses large data sets from variety of satellites at different orbits ranging from LEO up to 40 Re (1 Re = 6371 km) in the magnetosphere behind the Earth. As seen in Eq. (10), $\mathbf{B}_{\mathrm{ext}}$ includes magnetic fields generated from different external sources like magnetospheric ring $\left(\mathbf{B}_{ring}\right)$, tail $\left(\mathbf{B}_{tail}\right)$, magnetopause $\left(\mathbf{B}_{mp}\right)$, and field aligned $\left(\mathbf{B}_{FC}\right)$ currents (Tsyganenko, 2002, 1995, 1989) in the magnetosphere.

Since the external magnetic field $\left(\mathbf{B}_{\mathrm{ext}}\right)$ is superimposed on the internal geomagnetic field, T89 gives the total geomagnetic field at the specified position. The magnetic activity level in T89 model is determined using the K_p index. It is calculated globally using magnetic field data from midlatitude magnetic stations at every 3-hours and expressed as the thirds of a unit, e.g. 2- is 1 2/3, 5o is 5 and 5+ is 5 1/3 ("Geomagnetic Kp and Ap Indices | NCEI," n.d.; Siebert and Meyer, 1996). One of the current issues related to T89 model in using it for spacecraft attitude purposes is about its inputs. T89 model acquires the magnetic index data such as K_p, AE, D_{st} etc. on board the spacecraft. It can be used during especially geomagnetically active times, for more accurate attitude estimations. These indices processed under T89 can be obtained from magnetic stations, and then sent to the spacecraft by telecommand signals. In this paper, we assumed to have this information every 3-hour without any delays. However, this might not be possible when the telecommand is not available for a portion of the orbital period. In such case, one solution is to prepare look-up tables for specific inputs as an alternative. Also, since T89 computes the external fields in addition to the internal fields from IGRF and sums those, its computational burden is heavier than the IGRF model.

2.3. Magnetometer Measurements

The magnetometers are the basic sensors at low Earth orbiting satellites for attitude determination purposes. The magnetometer measurements are modelled by using the geomagnetic field model vector that is transformed to the body frame and the measurement noise vector as,

$$\mathbf{B}_{m_k} = \mathbf{A}_k \mathbf{B}_{o_k} + \mathbf{v}_{B_k}, \tag{11}$$

where $\mathbf{B}_o$ is the magnetic field vector in orbit frame obtained from a geomagnetic field model, $\mathbf{B}_m$ is the magnetometer measurements in the spacecraft's body frame, $\mathbf{v}_B$ is the zero-mean Gaussian noise of the measurements. In this study, magnetometers are modeled so as to sense the external field based on the K_p index defined. For this purpose, T89 model is used for the magnetic field vector as $\mathbf{B}_{o_k} = \mathbf{B}_{o_k}^{\mathrm{T89}}$ to generate the magnetometer measurements.

3. Attitude Estimation Algorithm based on Kalman Type Filtering

An attitude estimation algorithm using Kalman type filter is seen in this section. The attitude states of the spacecraft can be estimated by using magnetometer measurements based filtering methods. For this purpose, a conventional extended Kalman filter is used in this study to show the effects of the external field and measurement noise levels on the attitude estimations. Fig. 1 shows the filtering procedure using geomagnetic field models and magnetometer measurements. The geomagnetic activity index is also included for taking the magnetic field anomalies into account. An EKF algorithm is used in this paper as the dynamics of the satellite's rotational motion and measurement models are nonlinear. We kept the filtering algorithm as a conventional EKF for focusing on the external effects and not the filtering extensions.

The attitude estimation problem can be expressed in terms of discrete-time nonlinear state-space model,

$$\mathbf{x}_k = f\left(\mathbf{x}_{k-1}\right) + \mathbf{w}_k, \tag{12}$$

$$\mathbf{y}_k = h_k\left(\mathbf{x}_k\right) + \mathbf{v}_k, \tag{13}$$

Here, $f(\cdot)$ is the system function and $h(\cdot)$ is the measurement function, $\mathbf{x}$ is composed of the state elements, $\mathbf{w}$ is zero-mean Gaussian noise with $\mathbf{Q}$, $\mathbf{y}$ is measurement vector, and $\mathbf{v}$ is a zero-mean Gaussian noise with $\mathbf{R}$. The state vector is composed of attitude angles and angular rates in this study. The measurement model used in the filter differentiates by scenarios in this study as $\mathbf{B}_{\text{IGRF}}$ for IGRF and $\mathbf{B}_{\text{T89}}$ for T89. However, the magnetometer measurements do not vary case to case and always sense the external field by using T89 model for the geomagnetic field vector.

The prediction and the update stages should be processed under EKF algorithm (Psiaki et al., 1990). The state vector can be estimated by,

$$\hat{\mathbf{x}}_k = \hat{\mathbf{x}}_{k|k-1} + \mathbf{K}_k \left\{\mathbf{y}_k - h\left(\hat{\mathbf{x}}_{k|k-1}\right)\right\} \tag{14}$$

The predicted vector is,

$$\hat{\mathbf{x}}_{k|k-1} = f\left(\mathbf{x}_{\mathbf{k}}\right) \tag{15}$$

The EKF's filter gain is,

$$\mathbf{K}_k = \mathbf{P}_{k+1|k}\mathbf{H}_k^T \left[\mathbf{H}_k\mathbf{P}_{k+1|k}\mathbf{H}_k^{\,T} + \mathbf{R}\right]^{-1} \tag{16}$$

where the measurement matrix is created using $\mathbf{H}_k = \dfrac{\partial h\left(\hat{\mathbf{x}}_{k|k-1}\right)}{\partial \hat{\mathbf{x}}_{k|k-1}}$.

This is an Author Accepted Manuscript version of the following article: D. Cilden-Guler, Z. Kaymaz, C. Hajiyev, Geomagnetic Storms in the Context of Spacecraft Attitude Estimation under Different Noise Levels. Advances in Space Research, 72(7), pp. 2733-2740, DOI: 10.1016/j.asr.2022.09.021, 2023.

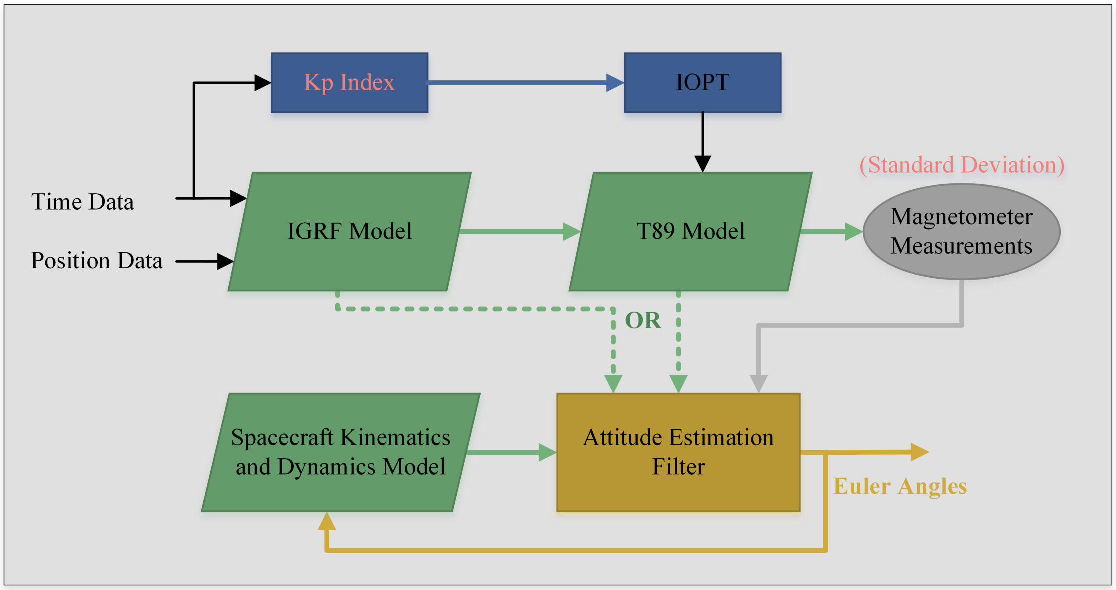

Fig. 1. Attitude estimation algorithm flow chart using magnetometer measurements.

The prediction error covariance matrix is,

$$\mathbf{P}_{k|k-1} = \frac{\partial f\left(\hat{\mathbf{x}}_k\right)}{\partial \hat{\mathbf{x}}_k} \mathbf{P}_{k-1|k-1} \frac{\partial f^T\left(\hat{\mathbf{x}}_k\right)}{\partial \hat{\mathbf{x}}_k} + \mathbf{Q} \tag{17}$$

The covariance matrix of the estimation error is,

$$\mathbf{P}_{k|k} = \left[\mathbf{I} - \mathbf{K}_k \mathbf{H}_k\right] \mathbf{P}_{k|k-1} \tag{18}$$

In this study, only magnetometer measurements are used as defined in (11),

$$\mathbf{y}_k = \mathbf{B}_{m_k} \tag{19}$$

The magnetic field model is used to compose the measurement matrix $\mathbf{H}_k$ within the filter.

4. Analysis and Results of the Case Studies

In the first setup, the simulations are run for a spacecraft with $\mathbf{J} = \mathrm{diag}\left(\left[2.1\times10^{-3} \quad 2.0\times10^{-3} \quad 1.9\times10^{-3}\right]\right)$ kg.m^2 principle mass moment of inertia that is tumbling along a low Earth circular orbit in the equatorial plane with 500 km altitude. The diagonal elements of the measurement noise covariance matrix are set to the square of standard deviation of the related sensor, and system noise covariance is set to

This is an Author Accepted Manuscript version of the following article: D. Cilden-Guler, Z. Kaymaz, C. Hajiyev, Geomagnetic Storms in the Context of Spacecraft Attitude Estimation under Different Noise Levels. Advances in Space Research, 72(7), pp. 2733-2740, DOI: 10.1016/j.asr.2022.09.021, 2023.

$\mathbf{Q} = \mathrm{diag}\left(\begin{bmatrix} 10^{-10} & 10^{-10} & 10^{-10} & 10^{-12} & 10^{-12} & 10^{-12} \end{bmatrix}\right)$. The simulation is initialized with the state vector of $\mathbf{x}_0^{\text{true}} = \begin{bmatrix} 0.03\ \text{deg} & 0.02\ \text{deg} & 0.01\ \text{deg} & 0.001\ \text{deg}/s & 0.0015\ \text{deg}/s & 0.002\ \text{deg}/s \end{bmatrix}^T$ and the filter is initialized as $\mathbf{x}_0^{\text{EKF}} = 2\mathbf{x}_0^{\text{true}}$. The simulations are performed for two orbital periods around 3 hours in total, and repeated for each magnetometer measurement noise standard deviation (σ) case and each K_p value. The orbit is propagated by employing the Simplified General Perturbation Version 4 (SGP4) model introduced by (Vallado and Crawford, 2008). The magnetometers are processed at 1 Hz and corrupted by Gaussian zero-mean noise with various standard deviations in nT. The simulations take the external field effects into account by implementing the various levels of K_p index.

The first part of this section focuses on the ratio between the external magnetic field and magnetometer measurement noise. The ratio is calculated using the norms of these vectors as $\|\mathbf{B}_{\text{ext}}\| / \|\mathbf{v}\|$ using predicted external field given by Eq. (10) and measurement noise given in Eq. (13). The ratio is presented as box plots for different activity levels and standard deviation value in different panels of Fig. 2. The boxplot has the data distribution of minimum, first quartile (bottom of the box), median (thin line in the box), third quartile (top of the box), and maximum. If the ratio is larger than 1, it means that the external field is greater than the noise, whereas the noise might cover the external effects for the rates that are smaller than 0.5. As reference lines, y-axis is marked with green at 0.5 and 1 in Fig. 2. The mean ratio is shown with a dark blue line. Selection of 0.5 is arbitrary just to give an easy reference guide.

The red box in Fig. 2 is created for determining the standard deviation level, where the noise mean is twice as large than the external field mean value. From this reference red box, one can determine the noise level that makes the external field less significant for attitude estimation purposes. However, it should be noted that the factor is arbitrarily chosen as 0.5 to be used as a guide. The white filled ellipse shape marks the first ratio value under 1.

Fig. 2.a shows the simulation performed under $K_p = 0$ that indicates absence of external magnetic field variations. The external field ratio over noise is reduced fast, and is masked after 60 nT magnetometer measurement noise standard deviation. The mean ratio follows an exponentially decreasing line.

This is an Author Accepted Manuscript version of the following article: D. Cilden-Guler, Z. Kaymaz, C. Hajiyev, Geomagnetic Storms in the Context of Spacecraft Attitude Estimation under Different Noise Levels. Advances in Space Research, 72(7), pp. 2733-2740, DOI: 10.1016/j.asr.2022.09.021, 2023.

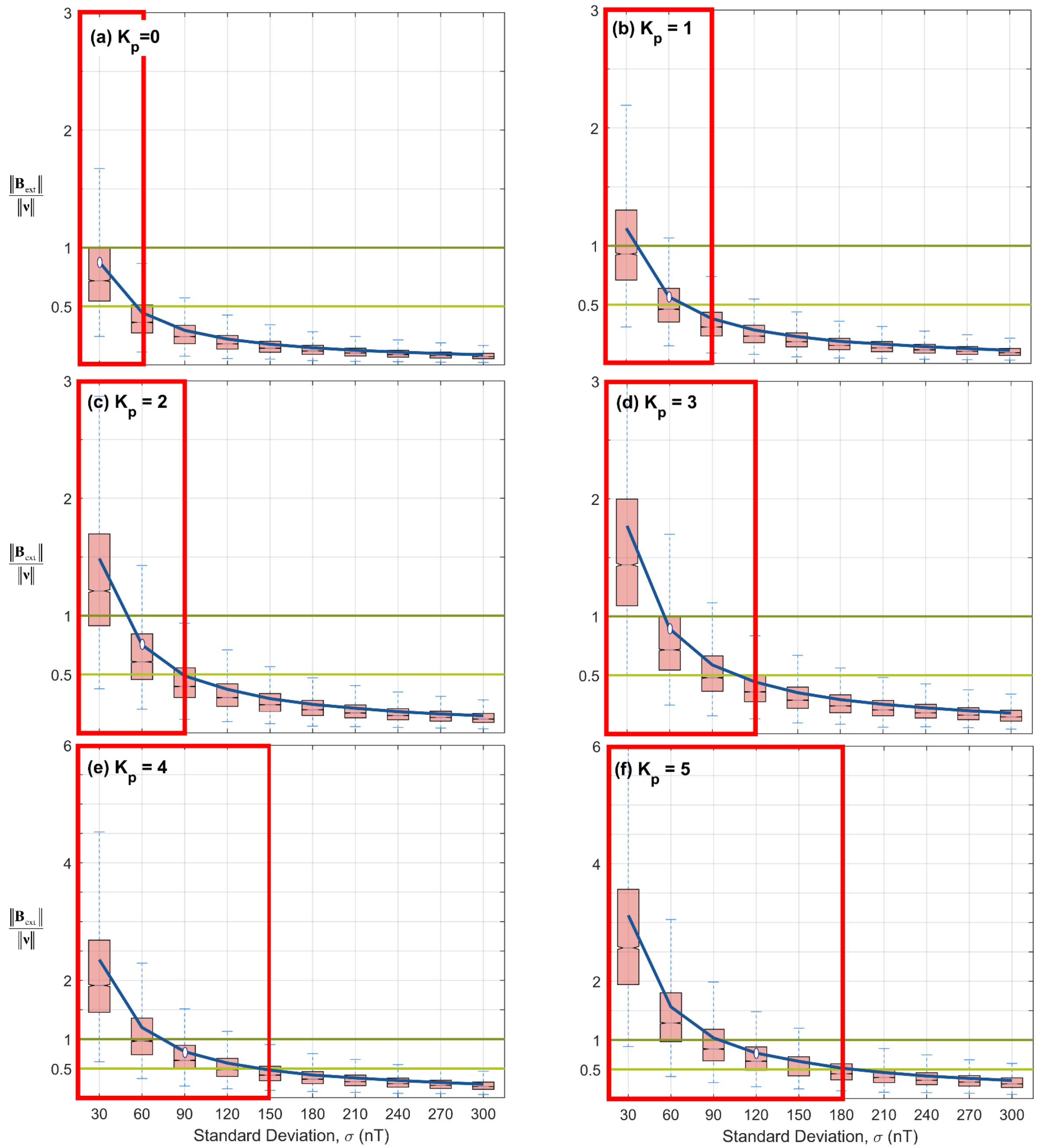

Fig. 2. Rate of the external field over noise on the magnetometer measurements. Note that the vertical scale is not the same in each panel (continued on the next page).

This is an Author Accepted Manuscript version of the following article: D. Cilden-Guler, Z. Kaymaz, C. Hajiyev, Geomagnetic Storms in the Context of Spacecraft Attitude Estimation under Different Noise Levels. Advances in Space Research, 72(7), pp. 2733-2740, DOI: 10.1016/j.asr.2022.09.021, 2023.

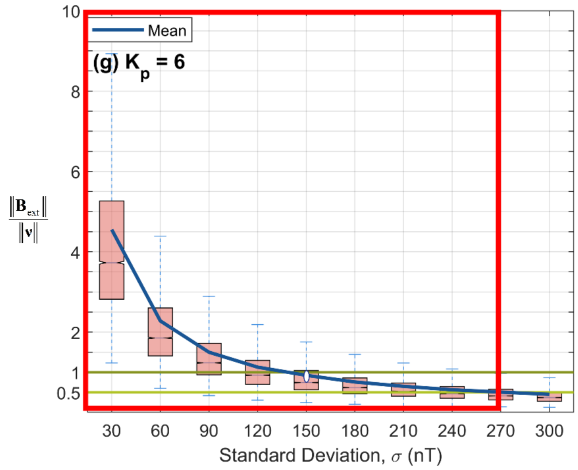

Fig. 2. Rate of the external field over noise on the magnetometer measurements. Note that the vertical scale is not the same in each panel (continued from the previous page).

The following panels give other cases with different K_p levels up to 6 which corresponds to the maximum magnetospheric activity level. The external effects are more effective up to the white filled ellipse than the measurement noise. The reference line 0.5 and the region in the red box in our case indicates that the external field still have an impact in the measurements. The region expands with larger K_p values. The corresponding standard deviation values are 60 nT, 90 nT, 90 nT, 120 nT, 150 nT, 180 nT, and 270 nT for $K_p = \{0 \quad 1 \quad 2 \quad 3 \quad 4 \quad 5 \quad 6\}$ respectively. This indicates that the external field can affect the magnetometer measurements that have noise levels with standard deviation up to 270 nT. It should be noted that the y axis limits are set differently for active times $(K_p \geq 4)$ and $K_p = 6$ in the panels of Fig. 2. The top quartiles of the box plots start to exceed the value 1 when $K_p \geq 4$. The mean value of the ratio also gets greater than 2. The external field is larger for 90 nT, 120 nT, and 150 nT standard deviation under $K_p = \{4 \quad 5 \quad 6\}$ respectively. From this result, it can be said that external magnetic field should be taken into account especially if the magnetometer measurement noise standard deviation is smaller than 150 nT. External field that is greater than the sensor noise will not be masked in the attitude determination procedure as an insignificant term. The differences in the strength of the magnetic field are found much smaller than those of magnetic field components (Cilden-Guler et al., 2018). Therefore, it can be stated that the geomagnetic storms have an effect on the attitude determination that is based on the angle between the directions of the reference and measurement vectors. The magnitude variations caused by geomagnetic storms without any directional changes would not affect the attitude performance as the attitude determination methods mostly use only the direction and not the magnitude in their computations.

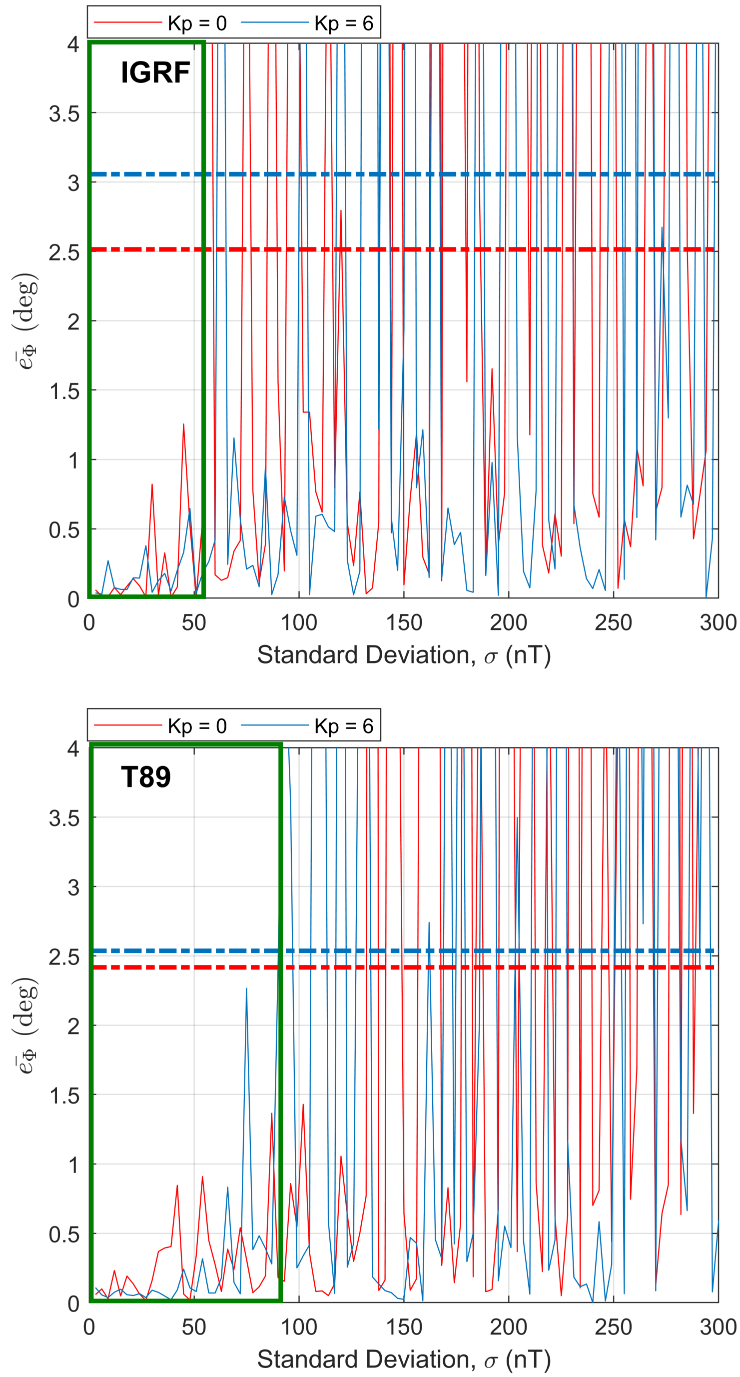

Fig. 3. The absolute error mean of the attitude estimation with two activity levels and varying noise using IGRF (top) and T89 (bottom).

This is an Author Accepted Manuscript version of the following article: D. Cilden-Guler, Z. Kaymaz, C. Hajiyev, Geomagnetic Storms in the Context of Spacecraft Attitude Estimation under Different Noise Levels. Advances in Space Research, 72(7), pp. 2733-2740, DOI: 10.1016/j.asr.2022.09.021, 2023.

The absolute mean attitude estimation errors after convergence along the orbit are calculated as $\bar{e}_{\Phi} = \sum_{k=1}^{N} \left\| \mathbf{x}_{\Phi_k}^{true} - \mathbf{x}_{\Phi_k}^{est} \right\| \Big/ N$ where $\mathbf{x}_{\Phi_k}^{true}$ is the true attitude angle vector, $\mathbf{x}_{\Phi_k}^{est}$ is the estimated attitude vector, and N is the number of samples after convergence are presented in Fig. 3. Two cases are considered for the simulation as IGRF or T89 implementation for the magnetic field model in the filter. There aren't any additional rules defined in the EKF design for the external field. The filter is tested against this case in its conventional form. Two activity levels are selected to see the difference in the estimation errors. Also, the mean values of the absolute mean attitude estimation errors are indicated with dotted dashed lines for both $K_p = \{0,\ 6\}$ as around 2.51 and 3.05 degrees for IGRF, 2.41 and 2.53 degrees for T89. The external field is only considered under the magnetometer measurements when the IGRF model is used. The mean value line of the attitude errors is only used as a limiting value to determine the green box's width before the first jump larger than the mean values of each figure. The corresponding standard deviations are around 50 nT and 100 nT for IGRF and T89 cases. These are critical points of the magnetometer noise levels that affect the attitude estimations abruptly. Another important point is that the mean error difference between $K_p = 0$ and $K_p = 6$ cases becomes smaller when using T89, as it considers the activity levels within the model. When the standard deviation is approaching to zero, in case of $K_p = 6$, the attitude estimation errors are under 0.1 deg. From the results, the measurement noise has more significant effect on the attitude estimation than the external field depending on the standard deviation level. The most significant conclusion from this figure is that one can decide the acceptable noise level for a given sensor with specified pointing requirement. For example, if T89 model is used on a spacecraft with 1-degree pointing requirement during a quiet time, then one can use a magnetometer with a standard deviation up to ~70 nT. For active times, it is ~80 nT for T89 and ~50 nT for IGRF. Here, T89 gives more room for the magnetometer selection. The variations in the standard deviation affect the estimation results significantly as seen in the figure as an abrupt change at the critical point that starts to mask the external field effects.

5. Conclusions and Discussion

In this study, the geomagnetic field models used in estimating the spacecraft's attitude angles are presented during geomagnetically active and quiet times. Magnetic field models commonly used for spacecraft attitude determination and control systems do not consider the external fields and thus the system might misinterpret the field anomalies as noise/ bias on the sensor, whereas the variations are caused by storm events, and not from the sensor itself. The external magnetic fields are detected by the magnetometer sensors; therefore, one of the geomagnetic models is selected so that it would take the magnetic anomalies into account. Here, the important point is that the level of the external magnetic field disturbance or the magnetometer noise that can vary depending on the sensor or strength of the external event. In order to see the effects of the external field and the measurement noise, a series of magnetometer sensor noise levels are applied under various magnetic activity levels.

This is an Author Accepted Manuscript version of the following article: D. Cilden-Guler, Z. Kaymaz, C. Hajiyev, Geomagnetic Storms in the Context of Spacecraft Attitude Estimation under Different Noise Levels. Advances in Space Research, 72(7), pp. 2733-2740, DOI: 10.1016/j.asr.2022.09.021, 2023.

A critical magnetometer noise level was previously presented in (Cilden-Guler et al., 2020) as 70 nT based upon one simulation case. However, in this study, it is shown that the external magnetic fields should be taken into account for the standard deviation of the measurement noise up to 150 nT. The external field can also be exposed and affect the results for the sensors having larger standard deviation value than 150 nT but not at the same level with those of smaller ones. The attitude estimation is influenced by the noise abruptly after approximately 50 nT and 90 nT for IGRF and T89 respectively. The mean error difference between $K_p = 0$ and $K_p = 6$ cases decreases when using T89 and comparing IGRF.

The presented results for determining the critical noise levels can be implemented on other systems, which are close enough to Earth and use magnetometer measurements for attitude determination purposes. Conventional EKF algorithm is used for attitude estimation in this study. For further work, other filtering algorithms can also be tested such as UKF, adaptive filters, particle filters etc.

Acknowledgement

We thank Prof. Dr. Nikolai Tsyganenko for sharing the most updated version of his models.

References

Carletta, S., Teofilatto, P., Farissi, M., 2020. A Magnetometer-Only Attitude Determination Strategy for Small Satellites: Design of the Algorithm and Hardware-in-the-Loop Testing. Aerospace 7(1), 3. doi:10.3390/aerospace7010003

Cilden-Guler, D., Kaymaz, Z., Hajiyev, C., 2021. Geomagnetic disturbance effects on satellite attitude estimation. Acta Astronaut. 180, 701–712. doi:10.1016/j.actaastro.2020.12.044

Cilden-Guler, D., Kaymaz, Z., Hajiyev, C., 2020. Are External Magnetic Disturbances Suppressed by Magnetometer Noise when Estimating a Nanosatellite's Rotational Motion?, IFAC-PapersOnLine, 53(2), pp. 14888-14893. doi:10.1016/j.ifacol.2020.12.1948

Cilden-Guler, D., Kaymaz, Z., Hajiyev, C., 2019. Assessment of Magnetic Storm Effects under Various Magnetometer Noise Levels for Satellite Attitude Estimation, in: 9th International Conference on Recent Advances in Space Technologies (RAST). IEEE, pp. 769–773. doi:10.1109/RAST.2019.8767834

Cilden-Guler, D., Kaymaz, Z., Hajiyev, C., 2018. Evaluation of Geomagnetic Field Models using Magnetometer Measurements for Satellite Attitude Determination System at Low Earth Orbits: Case Studies. Adv. Sp. Res. 61, 513–529. doi:10.1016/j.asr.2017.10.041

Cui, F., Gao, D., Zheng, J., 2020. Magnetometer-based autonomous orbit determination via a measurement differencing extended Kalman filter during geomagnetic storms. Aircr. Eng. Aerosp. Technol. 92, 428–439. doi:10.1108/AEAT-03-2019-0053

Geomagnetic Kp and Ap Indices | NCEI [WWW Document], n.d. URL https://www.ngdc.noaa.gov/stp/GEOMAG/kp_ap.html (accessed 10.13.20).

Inamori, T., Hamaguchi, R., Ozawa, K., Saisutjarit, P., Sako, N., Nakasuka, S., 2016. Online Magnetometer Calibration in Consideration of Geomagnetic Anomalies Using Kalman Filters in Nanosatellites and Microsatellites. J. Aerosp. Eng. 29, 04016046. doi:10.1061/(ASCE)AS.1943-5525.0000612

Inamori, T., Nakasuka, S., 2012. Application of Magnetic Sensors to Nano and Micro-Satellite Attitude Control Systems, in: Magnetic Sensors - Principles and Applications. Editor: Kevin Kuang, InTech, London. Available at: https://www.intechopen.com/chapters/30945, doi:10.5772/34307

Lu, Y., Shao, Q., Yue, H., Yang, F., 2019. A Review of the Space Environment Effects on Spacecraft in Different Orbits. IEEE Access 7, 93473–93488. doi:10.1109/ACCESS.2019.2927811

Olsen, N., Albini, G., Bouffard, J., Parrinello, T., Tøffner-Clausen, L., 2020. Magnetic observations from CryoSat-2: calibration and processing of satellite platform magnetometer data. Earth, Planets Sp. 72, 48. doi:10.1186/s40623-020-01171-9

Psiaki, M.L., Martel, F., Pal, P.K., 1990. Three-axis attitude determination via Kalman filtering of magnetometer data. J. Guid. Control Dyn. 13, 506–514. doi:10.2514/3.25364

Schulz, L., Heinisch, P., Richter, I., 2019. Calibration of Off-the-Shelf Anisotropic Magnetoresistance Magnetometers. Sensors 19, 1850. doi:10.3390/s19081850

Siebert, M., Meyer, J., 1996. Geomagnetic Activity Indices, in: Dieminger, W., Hartmann, G.K., Leitinger, R. (Eds.), The Upper Atmosphere. Springer Berlin Heidelberg, pp. 887–911. doi:10.1007/978-3-642-78717-1_26

Soken, H.E., Sakai, S. ichiro, 2020. Attitude estimation and magnetometer calibration using reconfigurable TRIAD+filtering approach. Aerosp. Sci. Technol. 99, 105754. doi:10.1016/j.ast.2020.105754

Thébault, E., Finlay, C.C., Beggan, C.D., Alken, P., Al., E., 2015. International Geomagnetic Reference Field: the 12th generation. Earth, Planets Sp. 67, 79. doi:10.1186/s40623-015-0228-9

Tsyganenko, N.A., 2002. A model of the near magnetosphere with a dawn-dusk asymmetry 1. Mathematical structure. J. Geophys. Res. Sp. Phys. 107, SMP 12-1-SMP 12-15. doi:10.1029/2001JA000219

Tsyganenko, N.A., 1995. Modeling the Earth's Magnetospheric Magnetic Field Confined within a Realistic Magnetopause. J. Geophys. Res. 100, 5599–5612.

Tsyganenko, N.A., 1989. A Magnetospheric Magnetic Field Model with a Warped Tail Current Sheet. Planet. Sp. Sci. 37, 5.

Vallado, D.A., Crawford, P., 2008. SGP4 orbit determination, Presentation at AIAA/AAS Astrodynamics Specialist Conf. Code, Honolulu, Hawaii. Available at:

"http://www.centerforspace.com/downloads/". doi:10.2514/6.2008-6770

Wertz, J.R., 2002. Spacecraft Attitude Determination and Control, Astrophysics and Space Science Library. D.Reidel Publishing Company, Dordrecht, Holland.

Zhang, Z., Xiong, J., Jin, J., 2015. On-orbit real-time magnetometer bias determination for micro-satellites without attitude information. Chinese J. Aeronaut. 28, 1503–1509. doi:10.1016/J.CJA.2015.08.001